AD-A060 251 ARMY ENGINEER TOPOGRAPHIC LABS FORT BELVOIR VA F/G 5/8
DELTA PULSE CODE MODULATION COMPRESSION RELATIVE TO STEREO IMAG--ETC(U)
SEP 78 M A CROMBIE

UNCLASSIFIED ETL-0157 NL

1 OF 1
AD A060251

END
DATE FILMED
12-78
DDC

ETL-0157

Delta pulse code modulation compression relative to stereo image matching

Michael A. Crombie

LEVEL II

SEPTEMBER 1978

U.S. ARMY CORPS OF ENGINEERS
ENGINEER TOPOGRAPHIC LABORATORIES
FORT BELVOIR, VIRGINIA 22060

78 10

ETL

Destroy this report when no longer needed.
Do not return it to the originator.

The findings in this report are not to be construed as an official Department of the Army position unless so designated by other authorized documents.

The citation in this report of trade names of commercially available products does not constitute official endorsement or approval of the use of such products.

UNCLASSIFIED

SECURITY CLASSIFICATION OF THIS PAGE (When Data Entered)

REPORT DOCUMENTATION PAGE	READ INSTRUCTIONS BEFORE COMPLETING FORM
1. REPORT NUMBER: ETL-0157	2. GOVT ACCESSION NO. / 3. RECIPIENT'S CATALOG NUMBER
4. TITLE (and Subtitle): DELTA PULSE CODE MODULATION COMPRESSION RELATIVE TO STEREO IMAGE MATCHING.	5. TYPE OF REPORT & PERIOD COVERED: Research Note.
	6. PERFORMING ORG. REPORT NUMBER
7. AUTHOR(s): Michael A. Crombie	8. CONTRACT OR GRANT NUMBER(s)
9. PERFORMING ORGANIZATION NAME AND ADDRESS: U.S. Army Engineer Topographic Laboratories, Fort Belvoir, VA 22060	10. PROGRAM ELEMENT, PROJECT, TASK AREA & WORK UNIT NUMBERS: 63701BR3202BB20
11. CONTROLLING OFFICE NAME AND ADDRESS: U.S. Army Engineer Topographic Laboratories, Fort Belvoir, VA 22060	12. REPORT DATE: September 1978
	13. NUMBER OF PAGES: 31
14. MONITORING AGENCY NAME & ADDRESS (if different from Controlling Office): 34p.	15. SECURITY CLASS. (of this report): Unclassified
	15a. DECLASSIFICATION/DOWNGRADING SCHEDULE

16. DISTRIBUTION STATEMENT (of this Report)

Approved for public release;distribution unlimited

17. DISTRIBUTION STATEMENT (of the abstract entered in Block 20, if different from Report)

18. SUPPLEMENTARY NOTES

19. KEY WORDS (Continue on reverse side if necessary and identify by block number)

Delta Pulse Code Modulation (DPCM)
Correlation
Quantization
Linear Predictors
Compression

20. ABSTRACT (Continue on reverse side if necessary and identify by block number)

The effect of DPCM compression on stereo image matching is analyzed. It was determined for the aerial image used in the study that third order linear prediction is adequate and that DPCM compression does not introduce a bias in stereo matching. The standard error of mismatch for images compressed to one bit per pixel compared to 8-bit images is approximately two-thirds of a pixel spacing for each coordinate.

DD FORM 1 JAN 73 1473 EDITION OF 1 NOV 65 IS OBSOLETE

UNCLASSIFIED

SECURITY CLASSIFICATION OF THIS PAGE (When Data Entered)

403 192

LB

PREFACE

The work covered by this Research Note was conducted by the Computer Sciences Laboratory (CSL), U.S. Army Engineer Topographic Laboratories (ETL), Fort Belvoir, Virginia. It is part of an effort being carried out in CSL on digital image analysis under project No. 63701BR3202BB20, Photogrammetric Exploitation. Studies were conducted by Michael A. Crombie with computer programming assistance by Philip Lem.

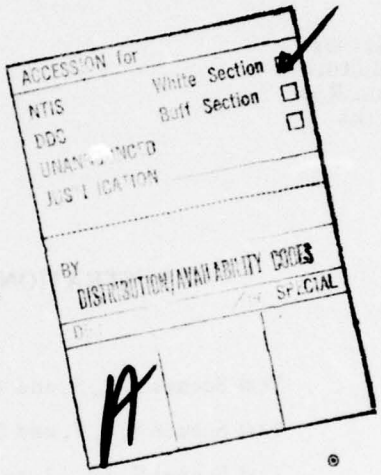

CONTENTS

ILLUSTRATIONS

TABLES

DELTA PULSE CODE MODULATION COMPRESSION RELATIVE TO STEREO IMAGE MATCHING

INTRODUCTION

The growing trend of collecting images in digital form and the associated requirement of processing the images interactively means that compression techniques will probably be employed to facilitate image transfer among image sensors and peripherals and to lessen the storage burden on image processors. This report presents an evaluation of the effect of compression on one image processing function, namely stereo image matching. The work is a continuation of a compression study that was reported on in a previous ETL Research Note.[1] In that Research Note, there was no information loss in the compression described, and consequently, there could be no adverse effect on image registration.

GENERAL METHOD

Delta Pulse Code Modulation (DPCM) with optimum quantization of gray shade differences was the technique used to compress the imagery, and conventional correlation methods were used to determine the effect of compression on image matching. The effect of compression on image matching was determined by noting the decrease in match precision as the level of compression increased.

Experimental Data

The 15 digitized stereo scene pairs used in this work were extracted from the Digital Image Analysis Lab (DIAL) system.[2] The scenes are displayed in appendix A along with specific digitizing information. Each scene was 125 by 125 pixels. The scenes are placed in order by REC01 signal power, that is, the signal power of scene 1 was larger than the signal power of scene 2, and so on. RECO1 is the DIAL label for the first of the two digitized stereo images.

Compression

Compression was achieved by quantizing the gray shade differences derived from DPCM. The differences are derived by predicting a gray shade at the source and then sending the difference between the actual gray shade and the predicted value. Differences are generally more independent than are the gray shades and their band width is less than the gray shade band width. As a result, these characteristics provide for more efficient data coding. The first step then is to determine a worthwhile linear predictor, and the next step is to derive an efficient quantization rule for an assigned number of bits per pixel.

Linear Predictor

Generally, a specific gray shade is predicted by a linear combination of prior gray shades, or prior gray shade estimates as in DPCM. The method of computing trial linear predictors is described in

---

[1] Michael A. Crombie, *Errorfree Compression of Digital Imagery*, U.S. Army Engineer Topographic Laboratories, Fort Belvoir, VA. ETL-0079, November 1976, AD-AO33 272.

[2] L. Gambino, B. Schrock "An Experimental Digital Interactive Facility," *Computer*, Vol.10, No.8, Aug.1977, p.22-28.

appendix B. It was assumed that the first line and the first column of gray shades of each scene were stored along with the quantized differences. Since the coefficients of the several trial linear predictors were derived by least squares, the mean squared error will be used to evaluate the predictors.

From the results shown in appendix B, a marked improvement in performance can be observed for higher order predictors as the scene signal power increases. However there is not much improvement to be gained in using fourth order predictors over third order predictors. In fact, there is not much improvement to be gained in using third order predictors over second order predictors for low signal power. Rather than complicate the work by varying the order of the predictor according to signal power, the third order predictor was used throughout. Note that specific third order coefficients were used for each of the 30 scenes.

Quantization — The digitized gray shades for the 30 scenes were represented by 256 levels (8 bits). The quantized gray shade differences were represented in turn by 1 to 6 bits. The numerical procedure for determining the 6 X 30 = 180 quantization rules is described in appendix C. In every case, the differences were derived by the pertinent third order linear predictor derived in appendix B.

DPCM — Assume that $(\alpha, \beta, \Upsilon)$ are the third order predictor coefficients. The quantity $g_{0,0}$ is defined as the predicted value of $g_{0,0}$ where $g_{0,0}$ is any one of the gray shades not in the first row or first column.

$$\bar{g}_{0,0} = \alpha * \tilde{g}_{0,-1} + \beta * \tilde{g}_{-1,0} + \gamma * \tilde{g}_{-1,-1}$$

$\tilde{g}_{K,L}$: Regenerated gray shades

(K,L) : Line and pixel indices

If $\bar{g}_{0,0}$ is the predicted value of $g_{0,0}$ then $d = g_{0,0} - \bar{g}_{0,0}$ is the difference and $\tilde{d}$ is the quantized difference. Finally, the regenerated gray shade is

$$\tilde{g}_{0,0} = \bar{g}_{0,0} + \tilde{d}$$

Since the quantized difference $\tilde{d}$ is inexact, the regenerated gray shade $\tilde{g}_{0,0}$ will be in error. The amount of error is directly related to the number of bits assigned to represent the true difference d. The error is given by the following equation:

$$\epsilon = g_{0,0} - \tilde{g}_{0,0}$$

Average errors and standard errors of ϵ for six scenes are presented in appendix C. Both the average errors and the standard errors decrease as the signal power decreases and as the number of bits assigned to d increases (see tables C5 and C6).

It is difficult to determine from the tabulated results of appendix C just what the adverse effect of a specific quantization rule is on an intended use of the imagery.

Image Matching

The object of this work was to determine the adverse effect of compression on stereo matching. This objective was accomplished by comparing compressed match results to 8-bit match results.

A 9 by 9 rectangular grid of points was designated on each of the 15 RECO1 scenes, and their corresponding points on the 15 RECO2 scenes were determined by conventional correlation methods. The defined points in the RECO1 scenes were spaced 10 pixels and 10 lines apart. A match point was estimated on the RECO2 scene, and an 11 by 11 correlation function was generated about the estimate. The line and pixel location of the correlation maximum was computed and designated as the match point. Note that the correlation function was computed at integer pixel and line intersections; whereas, the match point was computed to fractions of line and pixel values. This correlation function was calculated for each of the 9 X 9 = 81 defined points. Four different window sizes were used to generate the correlation functions.

Window Size (Pixels)	Ground Dimension (Feet)
7 x 7	24 x 24
11 x 11	40 x 40
17 x 17	64 x 64
21 x 21	80 x 80

Several precautions were taken to decrease the possibility of incorrect matches from procedure rather than from compression. The precautions along with a summary of match results are presented in appendix D.

DISCUSSION

The object of the numerical tests was to calculate the effect of one type of data compression, namely DPCM, on a specific photogrammetric function, that is, stereo image matching. The parameters of DPCM and the parameters of the K-bit quantization rule were adapted to local scene characteristics. Thus, the process should be near optimum in the type of compression and in the specific imagery.

Four estimates of each of the 81 match points for the 15 scene pairs were computed using the six K-bit quantized images and using the full 8-bit images. The four estimates

pertain to the four window sizes. Weighted averages of the match points were computed; the procedure is described in appendix D.

$$\bar{X}_{ISK},\ \bar{Y}_{ISK}$$

I = 1, 81 points

S = 1, 15 scene pairs

K = 1, 6 and 8 bits.

Table 1 shows the internal precision of the four estimates for six of the scenes and for the several K-bit images. The internal precision is simply the standard deviation in pixel spacing of the individual estimates (according to window size) with respect to the weighted averages. The first entry is the standard deviation in X, and the second is the standard deviation in Y. The scenes were organized according to signal power; scene 1 had the largest signal power and scene 15, the least.

Table 1. Internal Precision

	SCENE					
Bit	1	3	6	9	13	15
1	.75	1.03	.75	1.07	1.55	1.40
	1.42	1.74	.47	1.39	1.43	1.54
2	.55	.93	.73	.92	1.28	1.26
	1.62	1.59	.60	1.19	1.34	1.34
3	.57	1.13	.81	.96	1.18	1.14
	1.60	1.65	.53	1.22	1.12	1.27
4	.55	.97	.77	.88	1.27	1.25
	1.58	1.53	.54	1.11	1.28	1.38
5	.56	1.03	.71	.97	1.25	1.24
	1.53	1.62	.54	1.36	1.21	1.39
6	.55	.96	.76	.85	1.23	1.33
	1.57	1.59	.54	1.14	1.25	1.39
8	.54	1.03	.74	.87	1.19	1.21
	1.53	1.60	.53	1.16	1.22	1.39

In table 1, the internal precision does not appear to vary as the number of bits K increases or as signal power varies. The table does show that the internal precision in Y is less than (i.e. its standard error is larger) the internal precision in X. This is not unexpected since the major parallax direction is along the image Y-axis. In any case, the consistency of the internal precision over K and over signal power provided justification for comparing the K-bit weighted estimates to the 8-bit weighted estimates as a means for evaluating the K-bit compression.

The method for calculating the comparative results is described in appendix D, and results for six of the scenes are presented in tables D3 and D4. In table D3, the DPCM compression does not introduce a bias between K-bit and 8-bit match results.

In table D4, the standard error of the discrepancies between K-bit and 8-bit match results decreases as K increases. Also in table D4, the standard error of discrepancy does not vary as signal power varies. Since most of the information used in the correlation process is derived from the lower frequencies, the compression process functions like a low pass filter. For this reason, the results for the set of 15 scenes were combined to produce table 2.

The units in table 2 are pixel spacings. The quantity σ is a combined estimate of the standard error of discrepancy in X and Y.

Table 2. Weighted Averages of σ_{8K}

Bit	σx	σy	σ
1-8	0.554	0.758	0.664
2-8	0.487	0.466	0.476
3-8	0.265	0.313	0.290
4-8	0.222	0.189	0.206
5-8	0.171	0.178	0.174
6-8	0.150	0.149	0.150

The entries in table 2 pertain to standard errors of mismatch between K-bit images and 8-bit images. For example, the standard error between match results of 8-bit images and 1-bit images is about two thirds of a pixel spacing in each coordinate. The standard error is reduced to less than one fifth of a pixel spacing as K is increased to 6 bits.

The average number of bits per pixel can be reduced by efficient coding of the quantized differences, such as in Huffman coding.[3] If the average number of bits per pixel must be reduced to a small fraction of a bit, then either line and pixel thinning must be applied to the image before DPCM or transform coding methods must be employed. However, if the image processing facility can accommodate one or two bits per pixel, then DPCM will provide images that do not create a bias in stereo image matching, so that the standard error of mismatch between original results and results derived from compressed data is less than two thirds of a pixel in each coordinate.

CONCLUSIONS

1. The third order linear predictors are sufficiently precise for DPCM when applied to aerial imagery.
2. The DPCM compression does not introduce a bias in stereo matching.
3. The standard error of mismatch for images compressed to one bit per pixel by DPCM compared to fully resolved images is approximately two thirds of a pixel spacing for each coordinate.

---

[3]Michael A. Crombie, *Errorfree Compression of Digital Imagery*, U.S. Army Engineer Topographic Laboratories, Fort Belvoir, VA. ETL-0079, Nov 1976, AD-A033 272.

APPENDIX A. DIGITIZED SCENES

Fifteen digitized stereo scenes were extracted from the DIAL system for the compression analysis. The 15 scene pairs are subsets of a larger scene that was scanned on the PDS 1050A Automatic Microdensitometer system.[1] The pixel spacing and the line spacing was 24 μm (micrometers), the pixel diameter was 34.5 μm, and 256 gray shades (8 bits) were used to represent the image density.

The left image is referred to as RECO1 and the right image is referred to as RECO2. The RECO1 image scenes given below are photographic reproductions extracted from the DIAL COMTAL display. The central portion of each scene was used in the compression study.

Figure A1. Test Scenes 1,2,3, and 4.

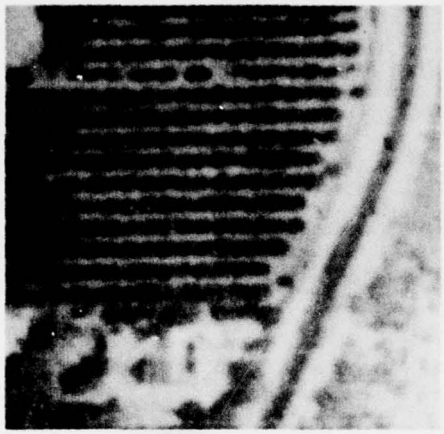

Scene 1

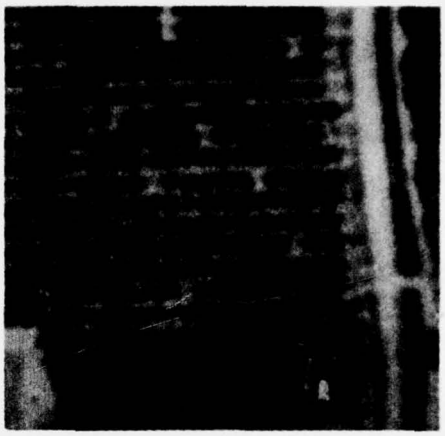

Scene 2

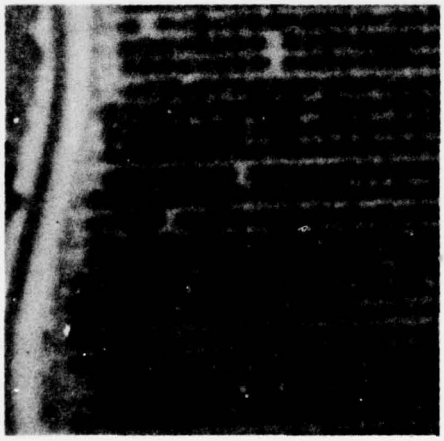

Scene 3

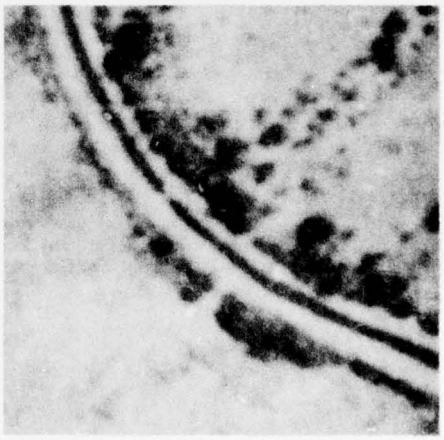

Scene 4

[1] **Michael A. Crombie,** *Stereo Analysis of a Specific Digital Model Sampled from Aerial Imagery*, U.S. Army Engineer Topographic Laboratories, Fort Belvoir, VA., ETL-0072, September 1976, AD-AO33 567.

Figure A2. Test Scenes 5,6,7, and 8.

Scene 5

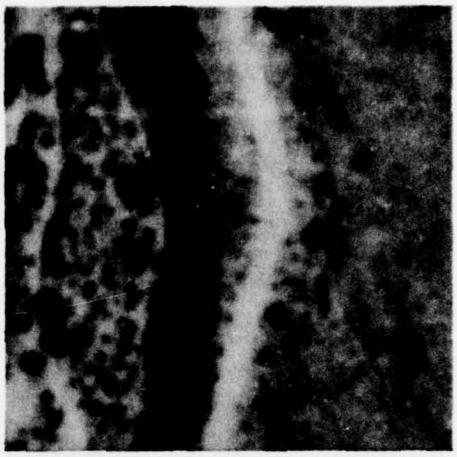

Scene 6

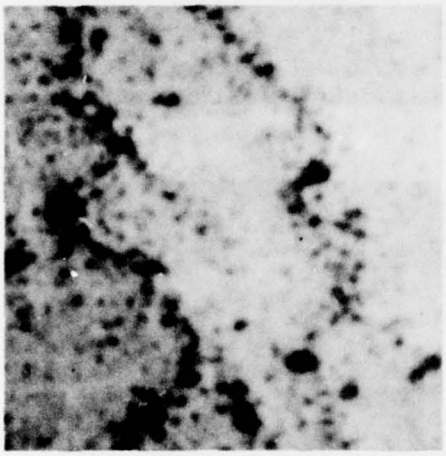

Scene 7

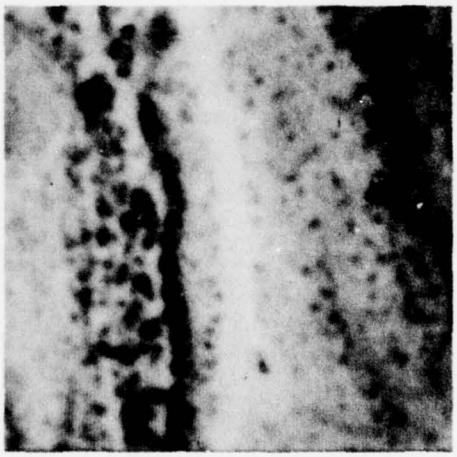

Scene 8

Figure A3. Test Scenes 9, 10, 11, and 12.

Scene 9

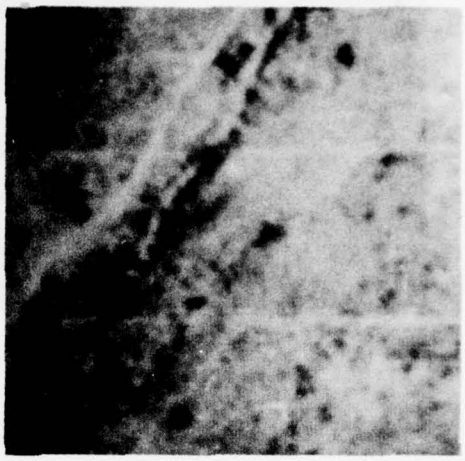

Scene 10

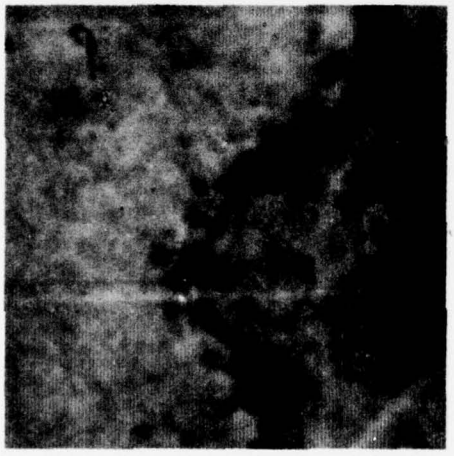

Scene 11

Scene 12

Figure A4. Test Scenes 13, 14, and 15.

Scene 13

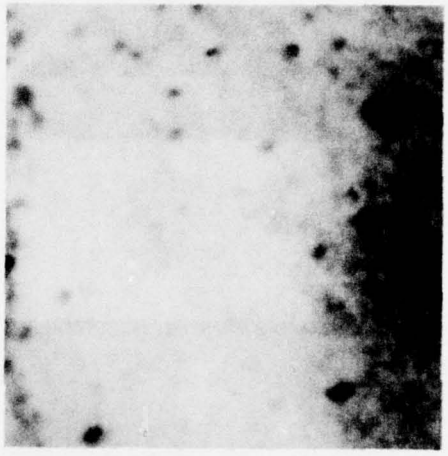

Scene 14

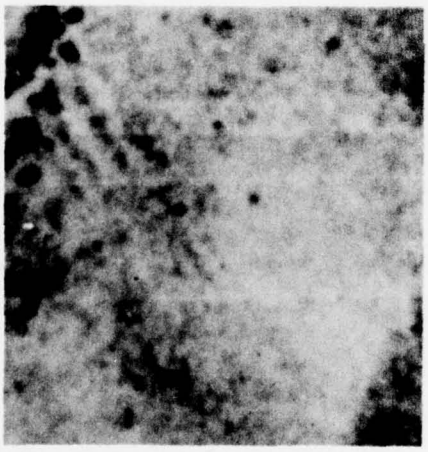

Scene 15

APPENDIX B, LINEAR PREDICTORS

Assume that the first line of an N^2 digital image is stored along with the first gray shade of each succeeding line. The remaining $(N-1)^2$ gray shades will be represented by coded differences. The difference d_{ij} for i and j >1 is the difference between the actual gray shade g_{ij} and a predicted value $\hat{g}_{ij}$.

$$\hat{g}_p = \sum_k a_k \, g_k$$

The subscript p pertains to any one of the $2 \leq (i,j) \leq N$ locations, and k pertains to one of the K predictor coefficients. The coefficients α_k are chosen so that the mean square error S is minimized.

$$S = \sum_p (\hat{g}_p - a_k \, g_k)^2$$

$$P = 1, P = (N-1)^2$$

The least squares solution for the α_k becomes a function of the digital image autocorrelation function. Five linear predictors are described next.

The following matrix represents the fifth order normalized autocorrelation function.

$$R = \begin{matrix} 1 & R_{01} & R_{02} & R_{03} & R_{04} & R_{05} \\ R_{10} & R_{11} & R_{12} & R_{13} & R_{14} & R_{15} \\ R_{20} & R_{21} & R_{22} & R_{23} & R_{24} & R_{25} \\ R_{30} & R_{31} & R_{32} & R_{33} & R_{34} & R_{35} \\ R_{40} & R_{41} & R_{42} & R_{43} & R_{44} & R_{45} \\ R_{50} & R_{51} & R_{52} & R_{53} & R_{54} & R_{55} \end{matrix}$$

The $(1,m)^{th}$ entry of R represents the normalized correlation between gray shades that are lagged (1 - 1) rows and (m - 1) columns. The normalization was achieved by dividing each element of the autocorrelation by Υ_{oo}, where Υ_{oo} is the image variance. In what follows, let $g_{o,o}$ represent the gray shade in question, i.e. any one of the $(N-1)^2$ values to be estimated.

First Order-Row

Assume that $g_{o,o}$ is to be estimated by the preceeding gray shade in the same line.

$$\hat{g}_{o,o} = \alpha \, g_{o,-1}$$

$$\alpha = R_{o1}$$

$$S = 1 - R_{o1}^2$$

The symbol S represents the normalized theoretical mean square error. The mean square error in all cases is

$$\sigma^2 = S * \Upsilon_{oo}$$

First Order - Column

Assume that $g_{o,o}$ is to be estimated by the preceeding gray shade in the same column.

$$\hat{g}_{o,o} = \beta\, g_{-1,0}$$

$$\beta = R_{1o}$$

$$S = 1 - R_{1o}^2$$

Second Order

Assume that $g_{o,o}$ is to be estimated by the preceeding gray shade in the same row and by the preceeding gray shade in the same column.

$$\hat{g}_{o,o} = \alpha\, g_{o,-1} + \beta\, g_{-1,0}$$

$$\begin{pmatrix} \alpha \\ \beta \end{pmatrix} = \begin{pmatrix} 1 & R_{11} \\ R_{11} & 1 \end{pmatrix}^{-1} \begin{pmatrix} R_{o1} \\ R_{1o} \end{pmatrix}$$

$$S = 1 - \alpha\, R_{o1} - \beta\, R_{1o}$$

Third Order

Assume that $g_{o,o}$ is to be estimated by the same gray shades used in the second order linear predictor, plus the preceeding diagonal gray shade of the previous line.

$$\hat{g}_{o,o} = \alpha\, g_{o,-1} + \beta\, g_{-1,o} + \gamma\, g_{-1,-1}$$

$$\begin{pmatrix} \alpha \\ \beta \\ \gamma \end{pmatrix} = \begin{pmatrix} 1 & R_{11} & R_{1o} \\ R_{11} & 1 & R_{o1} \\ R_{1o} & R_{o1} & 1 \end{pmatrix}^{-1} \begin{pmatrix} R_{o1} \\ R_{1o} \\ R_{11} \end{pmatrix}$$

$$S = 1 - \alpha\, R_{01} - \beta\, R_{10} - \gamma\, R_{11}$$

Fourth Order

Assume that $g_{o,o}$ is to be estimated by the same gray shades used in the third order predictor, plus the succeeding diagonal gray shade of the previous line. Note that the last gray shade of each line cannot be estimated with this predictor.

$$\hat{g}_{o,o} = \alpha\, g_{o,-1} + \beta\, g_{-1,o} + \gamma\, g_{-1,-1} + \delta\, g_{-1,1}$$

$$\begin{pmatrix} \alpha \\ \beta \\ \gamma \\ \delta \end{pmatrix} = \begin{pmatrix} 1 & R_{11} & R_{10} & R_{12} \\ R_{11} & 1 & R_{01} & R_{01} \\ R_{10} & R_{01} & 1 & R_{02} \\ R_{12} & R_{01} & R_{02} & 1 \end{pmatrix}^{-1} \begin{pmatrix} R_{01} \\ R_{10} \\ R_{11} \\ R_{11} \end{pmatrix}$$

$$S = 1 - \alpha\, R_{01} - \beta\, R_{10} - \gamma\, R_{11} - \delta\, R_{11}$$

Results from 6 of the 15 scenes were compiled and are presented in the following tables. The columns labeled d pertain to the average difference, σ^2 pertains to the theoretical variances, and ss^2 pertains to the computed variances of the differences. A difference is simply $d = g_{o,o} - \hat{g}_{o,o}$, the difference between the actual gray shade and the estimated gray shade.

TABLE B1 Prediction Results of Scene 1

RECO1

Order of Predictor	α	β	γ	δ	$\bar{d}$	σ^2	ss^2
1st (col)	.81				29	342	333
1st (row)	.91				14	181	182
2nd	.28	.69			5	151	126
3rd	.47	.77	-.28		6	141	93
4th	.47	.53	-.18	.20	-2	121	104

$\gamma_{oo}^2 = 1006$

Autocorrelation Function

1.00	.81	.50	.32	.35	.50
.91	.77	.50	.34	.36	.52
.75	.66	.42	.29	.33	.51
.61	.53	.33	.21	.28	.47
.52	.44	.24	.13	.21	.41
.44	.37	.17	.06	.13	.33

RECO2

Order of Predictor	α	β	γ	δ	$\bar{d}$	σ^2	ss^2
1st (col)	.81				32	297	298
1st (row)	.91				15	148	157
2nd	.27	.70			5	131	114
3rd	.44	.77	-.25		6	122	90
4th	.43	.56	-.16	.18	-2	113	97

$\gamma_{oo}^2 = 872$

Autocorrelation Function

1.00	.81	.51	.33	.34	.48
.91	.77	.51	.36	.38	.53
.75	.66	.45	.32	.36	.52
.61	.54	.36	.25	.30	.47
.50	.43	.25	.15	.21	.40
.41	.35	.17	.06	.12	.32

TABLE B2 Prediction Results of Scene 3

RECO1

Order of Predictor	α	β	γ	δ	$\bar{d}$	σ^2	ss^2
1st (col)	.81				27	301	302
1st (row)	.90				14	169	171
2nd	.31	.67			3	133	121
3rd	.61	.81	-.46		5	107	75
4th	.62	.68	-.42	.12	0	97	79

Autocorrelation Function

$\gamma_{oo}^2 = 886$

1.00	.81	.53	.42	.52	.73
.90	.75	.49	.38	.47	.68
.75	.63	.40	.29	.39	.60
.65	.54	.32	.22	.32	.54
.62	.51	.29	.19	.29	.51
.61	.50	.28	.17	.25	.47

RECO2

Order of Predictor	α	β	γ	δ	$\bar{d}$	σ^2	ss^2
1st (col)	.78				32	331	329
1st (row)	.90				14	161	167
2nd	.26	.71			4	127	130
3rd	.54	.81	-.39		6	110	98
4th	.54	.70	-.36	.11	1	110	98

Autocorrelation Function

$\gamma_{oo}^2 = 849$

1.00	.78	.48	.35	.45	.66
.90	.73	.46	.34	.44	.64
.76	.63	.39	.28	.38	.58
.66	.54	.31	.21	.30	.50
.60	.49	.26	.14	.24	.45
.57	.46	.22	.10	.19	.41

TABLE B3 Prediction Results of Scene 6

RECO1

Order of Predictor	α	β	γ	δ	$\bar{d}$	σ^2	ss^2
1st (col)	.93				12	80	87
1st (row)	.91				16	110	102
2nd	.58	.41			2	56	54
3rd	.76	.67	-.45		3	43	40
4th	.75	.49	-.39	.14	1	43	40

Autocorrelation Function

$\gamma_{oo}^2 = 613$

1.00	.93	.82	.73	.67	.63
.91	.86	.78	.71	.66	.63
.74	.73	.68	.64	.61	.59
.60	.59	.57	.56	.54	.53
.49	.49	.48	.48	.47	.47
.42	.41	.41	.41	.41	.40

RECO2

Order of Predictor	α	β	γ	δ	$\bar{d}$	σ^2	ss^2
1st (col)	.91				16	91	90
1st (row)	.89				20	111	101
2nd	.55	.43			4	61	55
3rd	.71	.63	-.37		5	50	43
4th	.70	.42	-.30	.18	1	50	44

Autocorrelation Function

$\gamma_{oo}^2 = 507$

1.00	.91	.76	.66	.59	.55
.86	.83	.72	.64	.58	.54
.69	.67	.61	.56	.53	.50
.52	.51	.49	.47	.45	.44
.41	.40	.38	.38	.37	.37
.32	.31	.30	.30	.30	.30

TABLE B4 Prediction Results of Scene 9

REC01

Order of Predictor	α	β	γ	δ	$\bar{d}$	σ^2	ss^2
1st (col)	.88				23	82	82
1st (row)	.90				19	72	72
2nd	.44	.54			5	49	46
3rd	.57	.64	-.25		7	49	40
4th	.56	.41	-.18	.21	1	45	41

Autocorrelation Function

$\gamma_{oo}^2 = 376$

1.00	.88	.71	.61	.54	.50
.90	.83	.70	.60	.54	.49
.75	.73	.65	.58	.53	.48
.65	.64	.60	.55	.52	.47
.59	.59	.56	.53	.50	.46
.55	.55	.53	.51	.49	.46

REC02

Order of Predictor	α	β	γ	δ	$\bar{d}$	σ^2	ss^2
1st (col)	.79				42	126	122
1st (row)	.86				29	92	89
2nd	.36	.59			9	72	65
3rd	.50	.68	-.24		12	64	59
4th	.49	.57	-.21	.12	6	64	59

Autocorrelation Function

$\gamma_{oo}^2 = 340$

1.00	.79	.58	.48	.43	.40
.86	.73	.57	.48	.43	.40
.68	.62	.52	.46	.42	.39
.56	.53	.47	.44	.41	.38
.49	.47	.43	.42	.40	.38
.46	.44	.42	.40	.38	.36

TABLE B5 Prediction Results of Scene 13

RECO1

Order of Predictor	α	β	γ	δ	$\bar{d}$	σ^2	ss^2
1st (col)	.83				29	73	70
1st (row)	.88				22	54	59
2nd	.39	.57			6	39	40
3rd	.54	.68	-.27		8	37	37
4th	.53	.56	-.24	.12	4	37	36

Autocorrelation Function

$Y_{oo}^2 = 235$

1.00	.83	.65	.54	.47	.42
.88	.77	.64	.54	.48	.43
.71	.66	.59	.52	.47	.43
.60	.57	.54	.50	.46	.43
.52	.51	.49	.48	.46	.43
.46	.46	.46	.46	.45	.44

RECO2

Order of Predictor	α	β	γ	δ	$\bar{d}$	σ^2	ss^2
1st (col)	.76				44	98	95
1st (row)	.80				36	80	83
2nd	.40	.54			12	61	59
3rd	.50	.61	-.20		15	59	56
4th	.49	.51	-.17	.13	9	57	55

Autocorrelation Function

$Y_{oo}^2 = 227$

1.00	.76	.53	.42	.36	.32
.80	.67	.51	.41	.35	.30
.61	.56	.47	.39	.33	.28
.49	.46	.41	.37	.32	.27
.41	.39	.37	.35	.31	.27
.36	.35	.34	.33	.31	.27

TABLE B6 Prediction Results of Scene 15

RECO1

Order of Predictor	α	β	γ	δ	$\bar{d}$	σ^2	ss^2
1st (col)	.85				27	35	36
1st (row)	.86				25	33	33
2nd	.46	.50			7	23	21
3rd	.57	.60	-.23		9	21	20
4th	.56	.43	-.18	.18	3	20	20

Autocorrelation Function

$\gamma_{oo}^2 = 129$

1.00	.85	.67	.56	.48	.43
.86	.78	.65	.55	.49	.44
.68	.66	.59	.53	.48	.45
.54	.54	.52	.49	.47	.45
.45	.46	.45	.45	.45	.44
.38	.39	.40	.41	.42	.42

RECO2

Order of Predictor	α	β	γ	δ	$\bar{d}$	σ^2	ss^2
1st (col)	.73				52	59	60
1st (row)	.78				43	50	49
2nd	.40	.52			14	37	37
3rd	.52	.61	-.22		17	35	35
4th	.51	.53	-.21	.10	12	35	34

Autocorrelation Function

$\gamma_{oo}^2 = 125$

1.00	.73	.51	.41	.36	.32
.78	.63	.47	.40	.35	.32
.55	.49	.41	.37	.35	.32
.43	.40	.36	.36	.35	.32
.36	.34	.32	.33	.34	.32
.32	.30	.29	.31	.32	.31

APPENDIX C. QUANTIZATION RULE

Assume that any one of the prediction schemes of appendix B produced a set of differences $\{dj : j = 1, (N-1)^2\}$ and that it is required that the set be compressed by quantization methods. The set of differences will be represented by a finite number of difference levels $q_1, q_2, \ldots q_m$ which will reduce the number of bits needed to describe the set and at the same time will allow for a reasonably accurate reconstruction of the original image. Let $d_1, d_2, \ldots, d_{m+1}$ represent the interval boundaries for the M-quantized differences. Determine the set of q values and the set of d values so that the mean squared error of the quantization is minimized.

$$S = \sum_{i=1}^{M} \int_{d_i}^{d_{i+1}} (d - q_i)^2 \, pr(d) dd$$

pr(d) is the probability of the occurrence of difference d.

The solution[1] is given by the following expressions:

$$d_i = (q_{i-1} + q_i)/2 \qquad i = 2,3,\ldots,M$$

$$q_i = \frac{\int_{d_i}^{d_{i+1}} d \; pr(d) dd}{\int_{d_i}^{d_{i+1}} pr(d) dd} \qquad i = 1,2,\ldots M$$

[1] J. Max, "Quantizing for Minimum Distortion," *IRE Transactions Information Theory*, V. IT-6, 1960.

An iterative numerical solution described by Rosenfeld[2] was used to determine the q values and the d values. A sample density function was constructed from the set of differences, and the trapezoidal rule was used for numerical integration. Note that d_1 and d_{m+1} are known; they are the largest and smallest of the set of differences.

A set of q values, a set of d values, and a set of relative frequency values were estimated for each of the 30 scenes (15 stereo pairs) and for bit assignments ranging from one bit to six bits. Each of the 6 * 30 = 180 quantization rules pertain to differences derived from third order predictors. The relative frequency data pertains to the probability density distribution of the differences over the quantization intervals. A representative quantization rule for the first four bit assignments was derived by averaging over the 15 scenes. These results are presented below. Note that the pertinent rule was used in the compression analysis, not the averaged rule. The expected value of Q is computed from $\sum QP(Q)$; note that the quantized differences are positively biased.

TABLE C1 Average Quantization Rule for 1 Bit

	RECO1			RECO2	
Z	Q	P	Z	Q	P
-00			-00		
4.33	-0.67	.4530	8.18	2.36	.4414
+00	9.33	.5470	+00	13.99	.5586
	E(Q) = 4.80			E(Q) = 8.86	

TABLE C2 Average Quantization Rule for 2 Bits

	RECO1			RECO2	
Z	Q	P	Z	Q	P
-00			-00		
-2.31	-6.43	.1253	0.47	-4.29	.1225
4.79	1.81	.3613	8.65	5.22	.3445
11.29	7.76	.3753	16.13	12.07	.3820
+00	14.81	.1381	+00	20.18	.1510
	E(Q) = 4.81			E(Q) = 8.93	

[2]A. Rosenfeld, *Digital Picture Processing*, Academic Press, New York, San Francisco, London, 1976, pg 102.

TABLE 3 Average Quantization Rule for 3 Bits

	RECO1			RECO2	
Z	Q	P	Z	Q	P
-00			-00		
-7.94	-11.61	.0356	-6.48	-10.68	.0302
-1.92	-4.27	.1086	0.45	-2.29	.0970
2.23	0.42	.1807	5.38	3.20	.1751
5.71	4.03	.2292	9.49	7.56	.2268
9.11	7.38	.2079	13.42	11.42	.2176
12.92	10.08	.1457	17.81	15.41	.1550
18.24	15.02	.0677	23.91	20.22	.0775
+00	21.47	.0246	+00	27.61	.0208
	E(Q) = 4.67			E(Q) = 8.75	

TABLE C4 Average Quantization Rule for 4 Bits

	RECO1			RECO2	
Z	Q	P	Z	Q	P
-00	·		-00		
-11.24	-14.62	.0178	-11.03	-15.03	.0119
-5.68	-7.85	.0532	-4.57	-7.03	.0378
-1.89	-3.51	.0942	-0.29	-2.11	.0686
1.02	-0.28	.1285	2.99	1.53	.0991
3.46	2.33	.1426	5.71	4.44	.1186
5.60	4.59	.1369	8.11	6.98	.1268
7.52	6.60	.1112	10.29	9.24	.1297
9.33	8.45	.0936	12.37	11.34	.1071
11.08	10.22	.0710	14.38	13.39	.0888
12.82	11.94	.0517	16.42	15.37	.0712
14.63	13.69	.0374	18.57	17.47	.0448
16.58	15.57	.0242	20.86	19.67	.0406
18.74	17.60	.0157	23.43	22.06	.0303
21.31	19.88	.0088	26.40	24.80	.0147
24.68	22.74	.0060	30.06	28.01	.0077
+00	26.63	.0040	+00	32.11	.0056
	E(Q) = 4.35			E(Q) = 8.68	

The quantities ξ and σ_ξ in tables C5 and C6 are the average error and standard error of gray shades regenerated from the specific quantization process. The first entry in each set pertains to RECO1, and the second entry pertains to RECO2. Results from 6 of the 15 scenes are presented. The errors are defined by the following relation.

$$\varepsilon_j = g_{0,0} - [\alpha *_j \tilde{g}_{0,-1} + \beta *_j \tilde{g}_{-1,0} + \gamma *_j \tilde{g}_{-1,-1} + \tilde{d}_j]$$

$\tilde{d}_j$: Quantized difference

${}_jg$: Regenerated gray shades

$g_{0,0}$: Correct gray shade

j = 1,6 Quantization Rules

TABLE C5 Average Quantization Errors

	Scene					
Bit	#1	#3	#6	#9	#13	#15
1	.79	.52	.18	.09	-.05	-.32
	.97	.42	.44	-.01	-.37	-.11
2	.08	.03	-.10	-.03	-.11	-.13
	-.07	-.11	-.12	-.06	-.05	-.05
3	-.02	-.08	-.05	-.09	-.11	-.09
	-.03	-.05	-.05	-.10	-.08	-.12
4	-.03	-.06	-.08	-.04	-.05	-.06
	-.05	-.05	-.07	.01	-.02	-.07
5	-.02	-.04	.09	-.04	.49	-.10
	-.03	.05	-.06	.02	-.05	-.06
6	-.01	-.03	-.08	-.05	-.02	-.07
	-.03	.00	-.07	.00	-.05	-.07

TARGET C6 Standard Error of Quantization Errors

Bit	Scene #1	#3	#6	#9	#13	#15
1	10.95	8.57	7.78	7.15	6.34	4.69
	10.70	9.43	7.62	8.16	7.05	5.01
2	4.41	3.38	3.26	3.16	3.51	2.40
	4.08	4.51	3.05	4.61	4.05	2.68
3	2.20	1.74	1.73	1.78	2.18	1.22
	1.98	2.82	1.53	1.64	2.71	1.60
4	1.33	1.07	1.41	0.93	1.31	1.16
	1.15	2.17	1.08	1.75	2.27	1.20
5	0.91	1.03	1.68	1.02	2.90	1.06
	0.79	2.09	1.02	1.51	2.02	1.17
6	0.75	0.90	1.27	0.83	1.00	0.90
	0.85	1.85	1.00	1.04	1.86	1.07

APPENDIX D. MATCH RESULTS

Numerical results from the match procedure described in the General Method section are presented in this appendix. Average match results are presented in tables D1 and D2 below for six scenes and for 1- to 8-bit images. An attempt was made to match 81 points in each scene using 21 by 21, 17 by 17, 11 by 11, and 7 by 7 windows. The first row of four values in each set are averages of successful match correlation values. The second row of four values in each set are averages of a confidence measure that is defined below. Finally, the third row of four values in each set are the numbers of successful matches. The four values pertain to the four window sizes, namely 21 by 21, 17 by 17, 11 by 11, and 7 by 7, in order.

The confidence measure is the product of the two partial derivatives of the correlation function with respect to x and y respectively. Both of these values must be negative for the correlation function to be concaved downward. If either of the partial derivatives were positive, the match point was rejected. If a computed shift was larger than one in abloslute value, then that match point was rejected. The product of the two partial derivatives is regarded as a confidence measure in that large values indicate a narrow, well defined correlation function; whereas, small values indicate a flatter less well defined correlation function.

Table D1 Average Match Results

Bit	1				3				6				9				13				15			
1	.838	.840	.868	.869	.754	.764	.772	.797	.875	.862	.826	.813	.731	.714	.695	.680	.499	.504	.505	.559	.453	.459	.484	.559
	.019	.021	.021	.041	.044	.047	.060	.091	.017	.021	.033	.055	.010	.014	.022	.047	.009	.012	.026	.065	.008	.011	.026	.062
	69	70	66	65	77	76	75	72	80	80	80	80	73	73	73	71	78	79	75	71	74	77	77	74
2	.822	.822	.857	.853	.746	.762	.772	.787	.878	.861	.829	.818	.730	.713	.688	.672	.496	.505	.502	.543	.437	.449	.471	.540
	.027	.030	.036	.053	.056	.060	.071	.101	.027	.031	.051	.072	.021	.025	.037	.062	.014	.018	.033	.073	.010	.016	.029	.063
	75	74	72	77	79	78	74	76	80	81	79	79	73	73	76	74	80	80	78	76	78	78	78	74
3	.822	.815	.861	.854	.747	.767	.773	.789	.878	.862	.830	.815	.732	.715	.689	.665	.506	.513	.509	.545	.442	.455	.480	.551
	.029	.033	.040	.057	.060	.064	.077	.105	.029	.034	.054	.073	.025	.028	.041	.067	.015	.020	.034	.076	.011	.017	.031	.069
	76	76	73	75	80	78	76	74	80	81	79	81	73	73	77	74	79	80	75	73	76	79	73	67
4	.825	.818	.848	.858	.747	.761	.774	.791	.880	.864	.825	.822	.736	.709	.683	.675	.510	.519	.515	.561	.447	.452	.478	.545
	.029	.033	.039	.057	.061	.065	.078	.109	.030	.035	.054	.076	.026	.029	.042	.072	.015	.021	.036	.079	.012	.017	.030	.065
	77	76	76	76	79	78	76	75	80	81	81	78	72	75	77	71	79	79	77	73	75	78	74	70
5	.824	.822	.849	.859	.750	.761	.775	.792	.880	.864	.826	.824	.736	.711	.688	.672	.512	.519	.519	.556	.441	.452	.481	.546
	.029	.033	.039	.057	.062	.065	.078	.110	.029	.034	.053	.075	.026	.029	.042	.069	.015	.020	.033	.072	.012	.016	.031	.065
	77	76	75	76	78	77	76	74	80	81	81	79	72	75	76	74	80	79	76	77	76	79	74	70
6	.825	.819	.847	.862	.748	.760	.775	.791	.880	.864	.830	.827	.737	.722	.689	.672	.508	.517	.515	.551	.449	.452	.486	.643
	.029	.033	.040	.057	.061	.065	.078	.110	.030	.035	.054	.077	.027	.030	.043	.069	.015	.021	.039	.074	.012	.017	.031	.062
	76	78	75	76	79	77	76	75	80	81	80	77	72	73	76	73	79	80	77	74	74	78	73	71
7	.823	.818	.848	.860	.745	.758	.773	.791	.879	.863	.830	.826	.741	.722	.694	.671	.506	.517	.515	.555	.434	.448	.481	.553
	.029	.033	.039	.058	.061	.065	.080	.112	.030	.035	.054	.073	.027	.030	.043	.070	.015	.021	.037	.075	.012	.018	.031	.066
	77	78	76	74	79	77	75	75	80	81	80	79	71	73	75	74	79	80	77	75	80	78	72	68

Table D2 Average Match Results

A linear combination of the four or less match point estimates was computed for each point.

$$\bar{X}_{I,S} = \sum_{J=1}^{4} W_J \, X_{IJS}$$

$$\bar{Y}_{I,S} = \sum_{J=1}^{4} W_J \, Y_{IJS}$$

$$\sum_{J=1}^{4} W_J = 1$$

I = 1, 81 points

S = 1, 15 scenes

J = 1, 4 Window Sizes

Numerical values were assigned to the W_J according to window dimension; larger windows were assigned larger weights. Although the smaller windows usually produced higher correlation values and sharper peaks than the larger windows, the likelihood of a false peak is also higher. Suppose, for example, that all four estimates of a particular point were acceptable. The weights in this case would be

$$21 \times 21 : \quad W_1 = 21^2/P = 0.49000$$

$$17 \times 17 : \quad W_2 = 17^2/P = 0.32112$$

$$11 \times 11 : \quad W_3 = 11^2/P = 0.13444$$

$$7 \times 7 : \quad W_4 = 7^2/P = 0.05444$$

$$P = 21^2 + 17^2 + 11^2 + 7^2 = 900$$

The same weight definition applies to the four situations where three of the estimates are considered successful. Any point with two or fewer successful matches was ignored.

The weighted estimates for the 1- to 6-bit images were compared in turn to the 8-bit image-weighted estimates. The average difference and the standard error of the difference were calculated for comparison.

$$\varepsilon_{XK8S} = \frac{1}{L} \sum_{i=1}^{81} (X_{ISK} - X_{IS8})$$

$$\sigma^2_{XK8S} = \frac{1}{L-1} \sum_{i=1}^{81} [(X_{ISK} - X_{IS8}) - \varepsilon_{XK8S}]^2$$

K = 1, 6 bits

S = 1, 15 scenes

I = 1, 81 points

A similar pair of equations were evaluated for the Y measurements. The value L is less than or equal to 81; the value is the number of points that are represented by valid estimates from both 8-bit and K-bit matches. Results for six scenes are presented in tables D3 and D4. In table D3, DPCM compression does not cause a bias between K-bit image match results and 8-bit image match results. In table D4, the standard error of the discrepancies between K-bit image matches and 8-bit matches decreases as K increases. Note the units of the tabular entries in both tables are pixel spacings.

TABLE D3 Standard Error of Discrepancies Between K-Bit Matches and 8-Bit Matches

	SCENE					
Bit	1	3	6	9	13	15
1-8	0.103	0.542	0.150	0.193	0.589	0.685
	0.691	1.061	0.158	0.420	0.611	0.733
2-8	0.045	0.458	0.101	0.097	0.390	0.375
	0.163	0.472	0.053	0.215	0.414	0.298
3-8	0.043	0.336	0.041	0.441	0.332	0.229
	0.489	0.435	0.024	0.353	0.219	0.216
4-8	0.014	0.310	0.042	0.045	0.298	0.259
	0.053	0.271	0.040	0.066	0.153	0.249
5-8	0.014	0.320	0.043	0.117	0.278	0.271
	0.049	0.100	0.019	0.092	0.165	0.302
6-8	0.016	0.307	0.040	0.061	0.259	0.250
	0.011	0.271	0.040	0.046	0.126	0.210

TABLE D4 Average Discrepancy Between K-Bit Matches and 8-Bit Matches

	SCENE					
Bit	1	3	6	9	13	15
1-8	-0.014	-0.131	-0.017	-0.059	0.144	0.002
	-0.059	-0.132	0.085	-0.005	0.064	0.146
2-8	-0.003	-0.015	-0.019	0.004	0.070	-0.022
	0.018	-0.075	0.053	0.006	-0.024	-0.006
3-8	0.000	-0.028	0.002	-0.071	0.028	0.018
	0.040	-0.048	0.008	0.029	0.024	0.015
4-8	0.002	-0.040	-0.003	-0.013	0.040	-0.001
	0.007	-0.052	-0.006	0.001	-0.008	-0.006
5-8	0.001	-0.025	-0.023	-0.031	0.018	-0.014
	-0.001	-0.019	-0.005	-0.003	-0.049	0.049
6-8	0.002	-0.035	-0.008	-0.013	0.031	0.037
	0.011	-0.031	0.000	0.006	-0.016	-0.000